Thomas von Arx[1]
Michael M. Bornstein[2]

[1] Department of Oral Surgery and Stomatology, School of Dental Medicine, University of Bern, Bern, Switzerland
[2] Department of Oral Health & Medicine, University Center for Dental Medicine Basel UZB, University of Basel, Basel, Switzerland

CORRESPONDENCE
Prof. Dr. Thomas von Arx
Klinik für Oralchirurgie und Stomatologie
Zahnmedizinische Kliniken der Universität Bern
Freiburgstrasse 7
CH-3010 Bern
Tel. +41 31 632 25 66
Fax +41 31 632 25 03
E-mail:
thomas.vonarx@zmk.unibe.ch

SWISS DENTAL JOURNAL SSO 130: 10–28 (2020)
Accepted for publication:
6 July 2020

The bifid mandibular canal in three-dimensional radiography: morphologic and quantitative characteristics

KEYWORDS
Anatomy
Mandibular canal
Bifid mandibular canal
CT
CBCT

SUMMARY

The mandibular canal is a prominent anatomical structure and of great clinical importance since it contains the inferior alveolar nerve. The clinician is advised to proceed cautiously in the vicinity of the mandibular canal to avoid any damage to its neurovascular content. Based on observations in dry mandibles, in panoramic radiographs, and recently in three-dimensional radiography, various anatomical variations of the mandibular canals have been described. One such variant is the so-called bifid mandibular canal (BMC). Embryologically, multiple canals develop and subsequently fuse to form a single mandibular canal; however, occasionally fusion fails or is incomplete resulting in one or multiple BMCs. Clinically relevant issues with regard to the BMCs include hemorrhagic or neurological disorders following damage to these aberrant canals. This literature review presents morphological and quantitative data about BMCs from studies using three-dimensional radiography, i.e. CT and/or CBCT. The reported frequencies of BMCs per patient ranged from 9.8 to 66.5% and per mandibular side from 7.7 to 46.5%. Gender, age or side predilection is currently inconclusive with regard to the occurrence of BMCs. Various types of BMCs have been described in the literature, such as retromolar, dental, forward, or buccolingual canals. BMCs may originate from the mandibular canal along its entire course, but bifurcation appears to be more frequent in the posterior compared to the anterior canal portions. Mean BMC length was reported to range from 10.2 to 16.9 mm, and mean BMC diameter from 0.9 to 2.3 mm. In conclusion, the presence of a BMC must be taken into consideration for treatment planning and anesthetic, endodontic, or surgical interventions in the mandible.

Introduction

The mandibular canal (MC), also called inferior dental (nerve) canal or inferior alveolar (nerve) canal, is a prominent anatomical structure in the mandible (von Arx & Lozanoff 2017). The MC is of great clinical importance since it conveys neurovascular components to all mandibular teeth, to the body of the mandible, as well as to the lower lip, chin, and vestibular soft tissues anterior to the mental foramen. Any (inadvertent) damage to the MC may result in sensitivity changes or bleeding complications possibly leading to legal actions. Therefore, the clinician should have a sound knowledge of the anatomy and must proceed cautiously in the vicinity of the MC.

Panoramic radiography remains the standard imaging method for visualization of the MC. However, in many cases radiographic detection of the canal is difficult in its entirety or also partially. Several radiographic studies have documented the poor visibility of the MC, in particular in its middle and anterior sections (Angelopoulos et al. 2008; Kamrun et al. 2013; Politis et al. 2013). In a study of 500 panoramic radiographs, the superior border of the MC was visible only in 37% (Pria et al. 2011). Even when using three-dimensional (3D) radiography, the MC failed to be detected in 18% of cross-sectional cone beam computed tomography (CBCT) images at the level of the first molar (de Oliveira et al. 2012). The same authors also showed that corticalization of the MC (as seen on CBCT images) was significantly associated with the degree of bone trabeculation within the mandibular body.

The MC extends from the mandibular foramen to the mental foramen, thus traverses the mandibular body obliquely from its medial inner aspect at the ramus to the lateral outer aspect in the premolar region. In the sagittal plane, the course of the MC shows a high degree of variability: linear, spoon-shape or elliptic (Liu et al. 2009). Consequently, the MC may be close to or distant to the root apices (Carter & Keen 1971; Kovisto et al. 2011; Bürklein et al. 2015).

With regard to the development of the MC, the so-called Meckel's cartilage forms the skeleton of the first (mandibular) branchial arch. Later, the major portion of that cartilage disappears, but some parts transform into the sphenomandibular ligament. The bilateral bodies of the mandible develop from ossification centers located lateral to the Meckel's cartilage and its accompanying neurovascular bundle. The presence of the inferior alveolar nerve has been postulated as being necessary to induce osteogenesis. The prior presence of the neurovascular bundle ensures the formation of the actual MC (Sperber 1981).

A more detailed insight into the development of the human MC has been presented by Chavez-Lomeli et al. (1996). In a unique study of 302 hemimandibles from the second half of the prenatal period, it was shown that the configuration of the developing MC reflected the pattern of innervation to the dentition. Initially, a canal appeared to the primary incisors, followed by a canal to the primary molars, and lastly by one or more canals to the first permanent molars. Each analyzed hemimandible of the most mature group always presented three canals that originated from separate openings on the lingual surface of the ramus and they were directed to the different tooth groups. The authors concluded that the MC develops from at least three separate canals (Chavez-Lomeli et al. 1996). Rapid bone remodeling usually results in fusion of the originally distinct canals, but failure of coalescence would result in a bifid MC (BMC) or trifid MC (TMC) (Fig. 1–3). The so-called retromolar canal, located posterior to the 2nd or 3rd molar, is another accessory bone canal in the mandible (von Arx & Lozanoff 2017).

Historic classifications of BMCs have been provided by Nortje et al. (1977) and by Langlais et al. (1985) (Tab. I). Both reports described distinctive varieties of BMCs large enough to be detected with panoramic radiographs. A newer classification was reported by Naitoh et al. (2009) based on CBCT data. The most recent classification of BMCs using CBCT was suggested by Luangchana et al. (2019) (Tab. II).

The clinical relevance of the BMC is its presence but difficulty to be detected with two-dimensional radiography. Due to the neurovascular content, the BMC poses a risk for the patient as well as a challenge to the clinician. Several case reports have described intra- or postoperative complications related to damage of the BMC (Maqbool et al. 2013; Aljunid et al. 2016; Verea Linares et al. 2016).

The objective of this article is to provide morphological and quantitative data of BMCs based on studies using 3D radiography (i.e. CT and/or CBCT).

Material and methods

The database "PubMed" (www.ncbi.nlm.nih.gov/pubmed) was searched for articles pertinent to BMCs. Furthermore, reference lists of papers about BMCs were screened for additional articles.

Some authors claim that the retromolar canal is a variant of the BMC (Naitoh et al. 2009; Orhan et al. 2011), while others consider this a separate entity since it has its own opening, i.e. the retromolar foramen. The retromolar canal might also have a different embryological background (Haas et al. 2016). For these reasons, articles limited to the retromolar canal were excluded for this evaluation.

Castro et al. (2015) provided a literature review about different classifications of BMCs. They concluded that 3D radiographic examinations appear to be the best method for identification of MC branching. Therefore, for the final analysis, only studies that provided morphological and/or quantitative data of the BMC based on 3D radiography (i.e. CT and/or CBCT) were included.

The following data with regard to BMCs were extracted:

- Classification of BMCs
- Frequency of BMCs per patient and/or per side (hemimandible)
- Number of BMCs
- Influence of gender, age or side on BMC frequency
- Location of BMC origin and its distance from the mandibular foramen
- Course of BMCs
- Length, diameter and angle of BMCs
- Distance from BMCs to root apices
- Corticalization of BMCs

Results

Classification of BMCs

The majority of 3D radiographic studies have used the BMC classification established by Naitoh et al. (2009) (Tab. II). Only few studies have applied the classifications based on panoramic views by Nortje et al. (1977) or by Langlais et al. (1985) even though the image analysis was done with CBCT scans.

Frequency of BMCs

A recent meta-analysis including only study samples > 300 has evaluated the frequency of BMCs including different evaluation

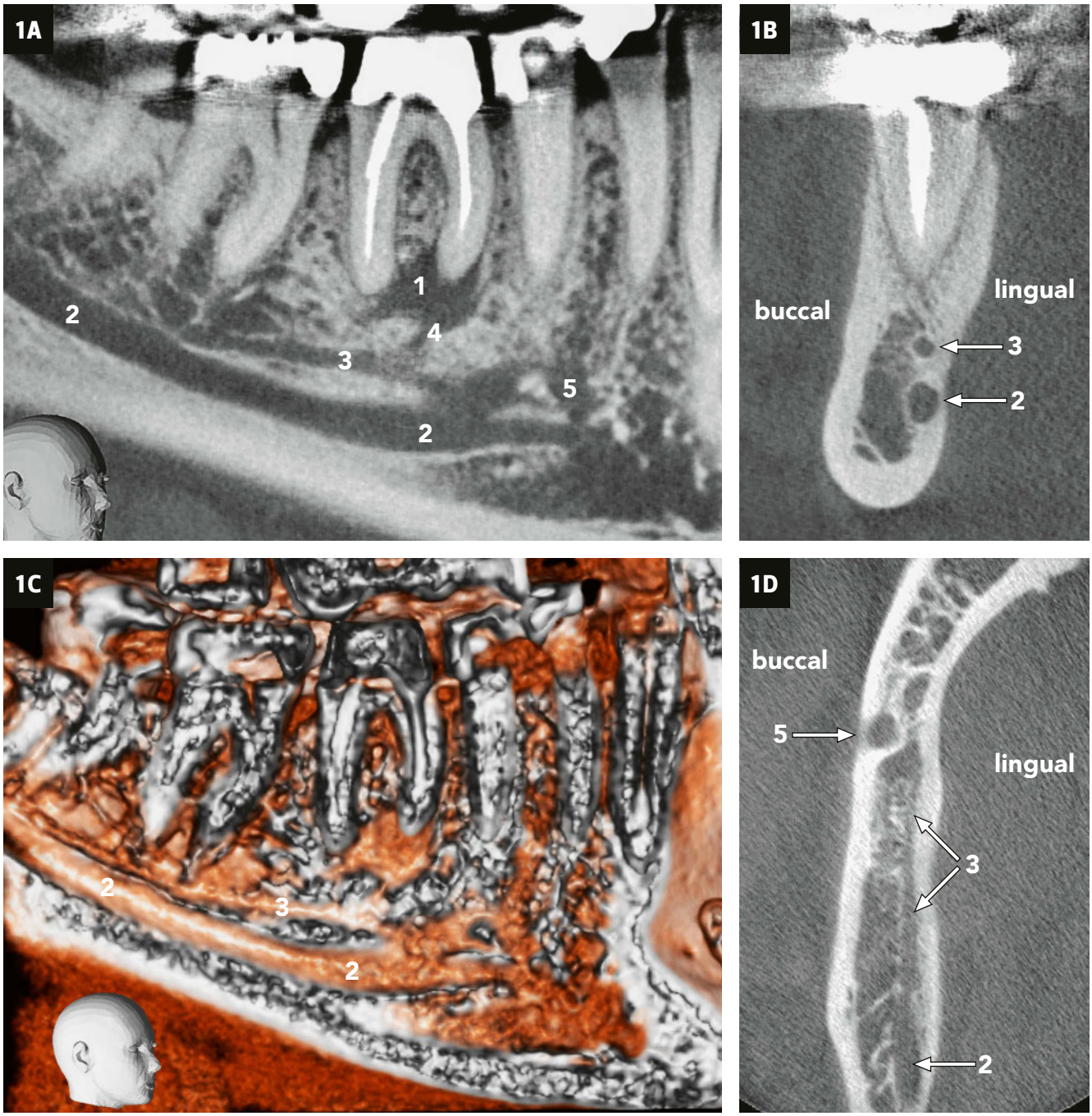

Fig. 1 CBCT assessment of a 68-year-old male referred for apical surgery of the lower right 1st molar (tooth 46). Sagittal image (A), coronal image at the level of the distal root of 46 (B), 3D-rendered image cut along MC and BMC (C), and axial image at the level of the mental foramen (D, inferior view).
1 = periapical lesion of mesial root of 46; 2 = MC; 3 = BMC; 4 = branch from BMC to mesial root of 46; 5 = mental foramen.

Fig. 2 CBCT assessment of a 62-year-old female referred for surgical removal of the retained lower left 3rd molar (tooth 38). A complex BMC configuration is present. Sagittal images (A–D), coronal image (E), 3D-rendered image (F, superior view), and axial image (G, inferior view).
1 = tooth 38; 2 = MC; 3 = BMC joining a retromolar canal; 4 = retromolar canal; 5 = retromolar foramen; 6 = two small BMCs arising from the retromolar canal and coursing anteriorly.

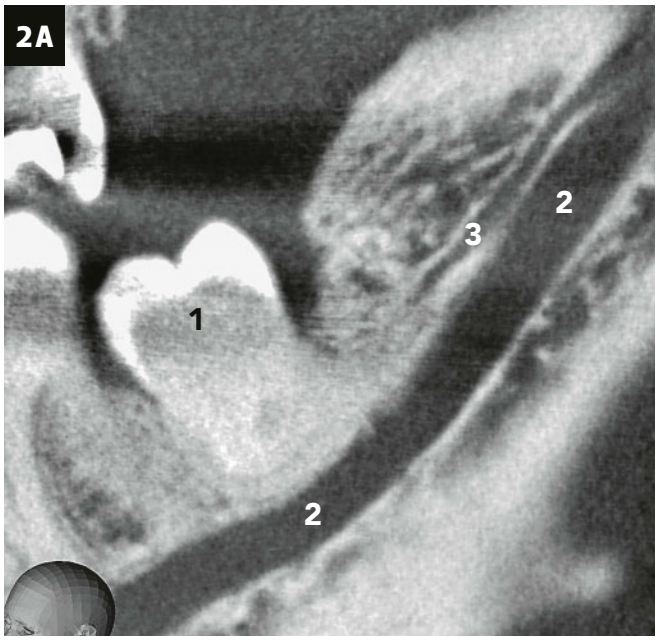
2A
1
3
2
2

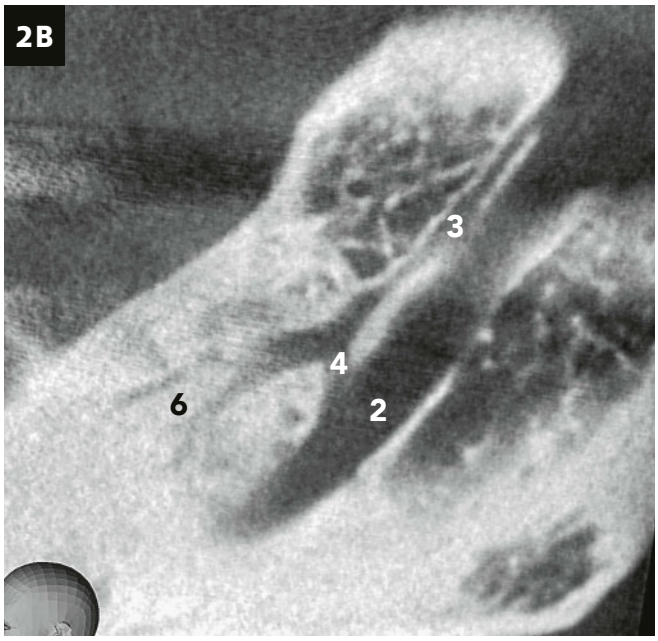
2B
3
4
6
2

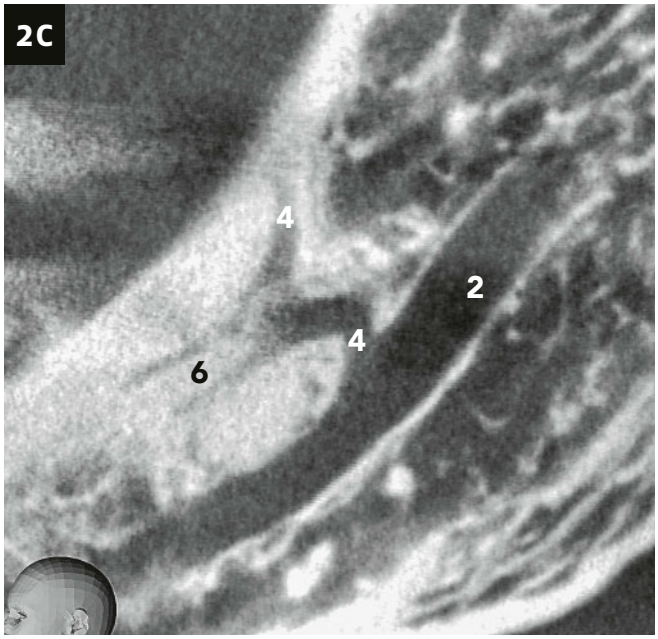
2C
4
2
4
6

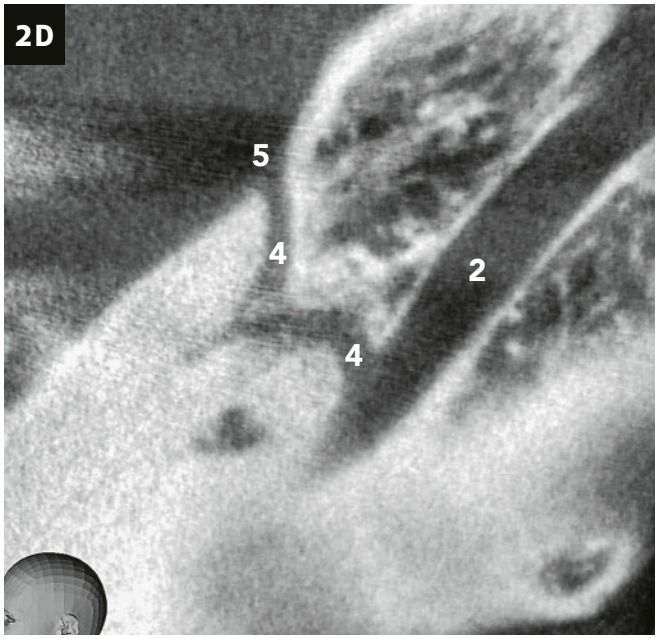
2D
5
4
2
4

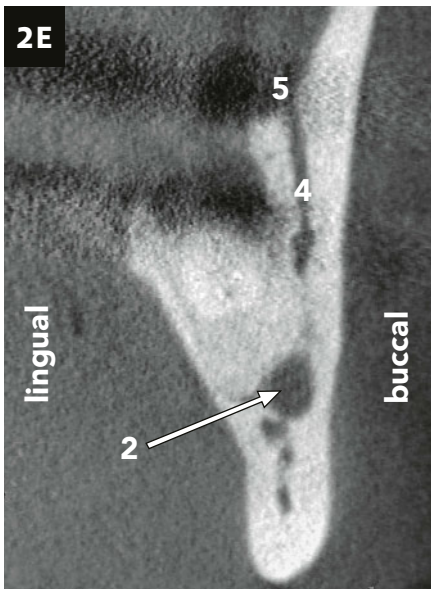
2E
5
4
lingual
buccal
2

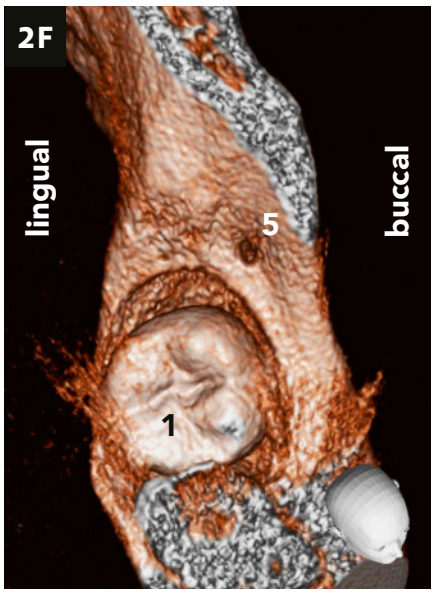
2F
lingual
buccal
5
1

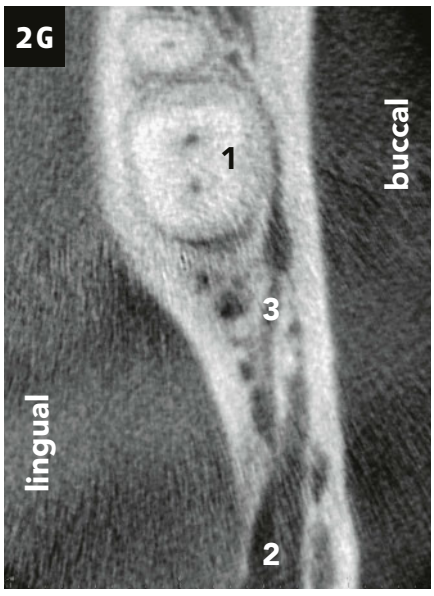
2G
1
buccal
3
lingual
2

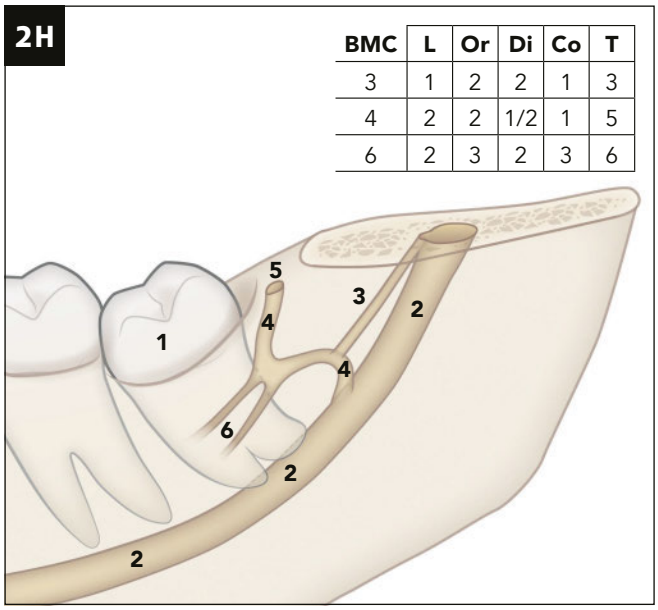

Fig. 2 CBCT assessment of a 62-year-old female referred for surgical removal of the retained lower left 3rd molar (tooth 38). A 3D illustration demonstrates the complex BMC courses (H): for **L–Or–Di–Co–T** numbers, refer to Table VIII.
1 = tooth 38; 2 = MC; 3 = BMC joining a retromolar canal; 4 = retromolar canal; 5 = retromolar foramen; 6 = two small BMCs arising from the retromolar canal and coursing anteriorly.

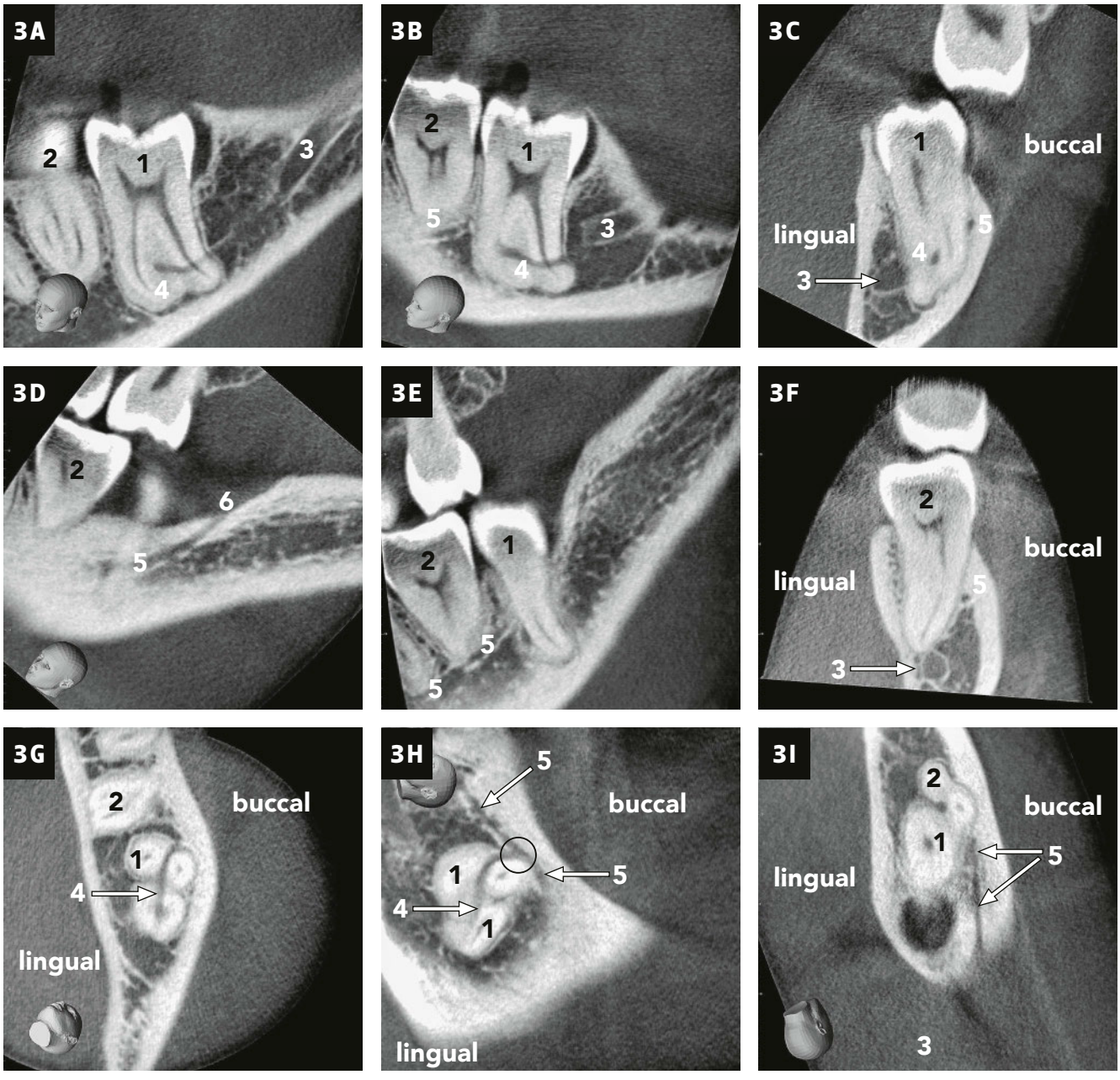

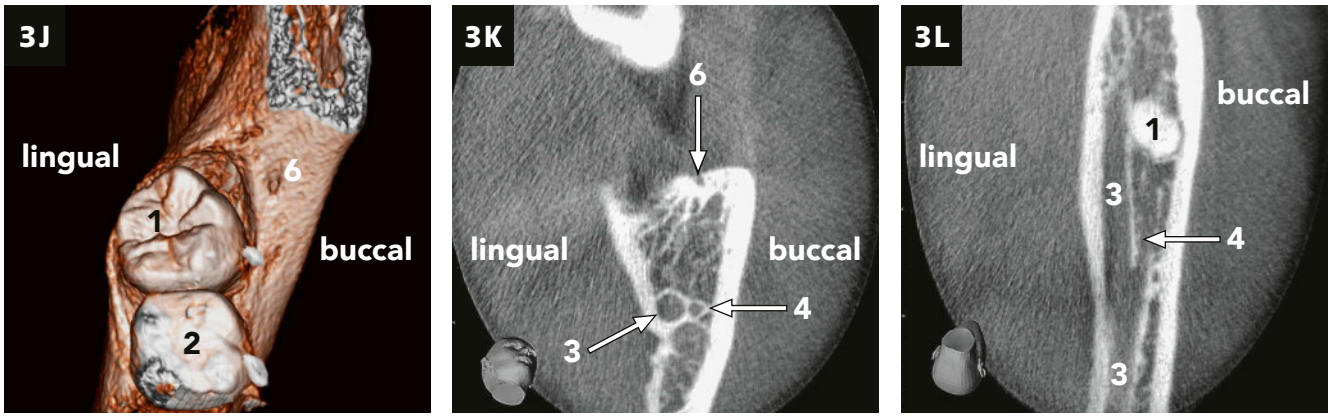

Fig. 3 30-year-old female presenting two BMCs. A lower BMC traverses the apical portion of the roots of the lower left 3rd molar (tooth 38). Then the accessory canal curves buccally to join an upper BMC running along the buccal root surfaces of teeth 38 and 37. The latter canal originates from a retromolar foramen. Sagittal images (A, B, D, E), coronal images (C, F, K), axial images (G, H, I, L, all inferior view), and 3D-rendered image (J, superior view). A 3D illustration demonstrates the complex BMC courses (M): for **L–Or–Di–Co–T** numbers, refer to Table VIII.
1 = tooth 38; 2 = tooth 37; 3 = MC; 4 = BMC traversing apical root portions of tooth 38; 5 = additional BMC running along the buccal aspects of teeth 37 and 38; 6 = retromolar foramen. In Fig. H, the circle ○ marks the site of BMC confluence.

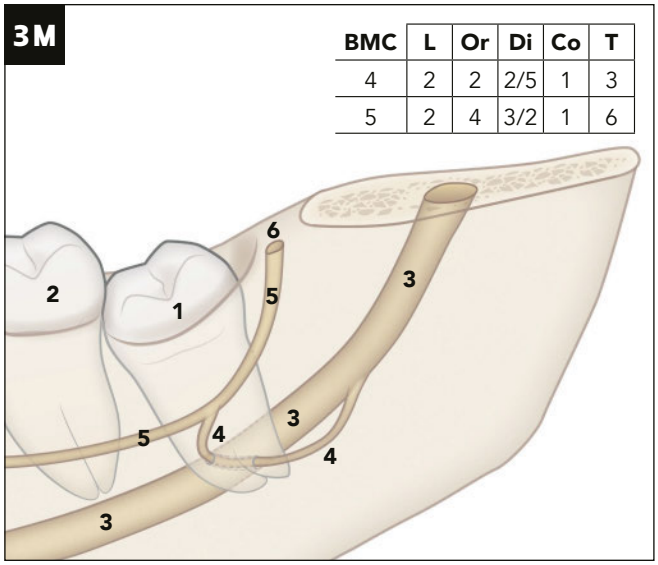

Tab. I Classification of BMCs

Author(s) and year *(imaging method)*	Classification	Definition
Nortje et al. 1977 *(panoramic radiography)*	Type I	Two canals originating from one mandibular foramen
	Type II	Short supplemental upper canal extending to 2nd or 3rd molar
	Type III	Two canals originating from two mandibular foramina, but joining together in the molar region to form one canal
	Type IV	Supplemental canal arising from the main canal and reaching the retromolar pad region
Langlais et al. 1985 *(panoramic radiography)*	Type 1	Uni- or bilateral BMC extending to 3rd molar or immediate surrounding area
	Type 2	Uni- or bilateral BMC extending along the course of the MC and rejoining it within the ramus or the body of the mandible
	Type 3	Combination of Type 1 on one side and of Type 2 on other side
	Type 4	Consists of two canals originating from separate mandibular foramina and then joining to form one larger MC
Naitoh et al. 2009 *(cone beam computed tomography)*	Type I	Retromolar canal: terminates at a foramen on the bone surface of the retromolar region
	Type II	Dental canal: extends to the root apex of 2nd or 3rd molar
	Type III	Forward canal: arising from superior MC wall other than Types I or II (with/without confluence to MC)
	Type IV	Buccolingual canal: originating from buccal or lingual wall of MC

BMC = bifid mandibular canal; MC = mandibular canal

Tab. I Classification of BMCs continued

Author(s) and year *(imaging method)*	Classification	Definition
Luangchana et al. 2019 *(cone beam computed tomography)*	Type A	Superior type: single or multiple canals branching superiorly from the main MC
	Type B	Forward type: BMC coursing forward and running lower than apices of teeth (B1 not merging, B2 merging with MC)
	Type C	Plexus type: branching plexus from MC
	Type D	Anterior extension type: branching from mandibular incisive canal (D1 single or series of canals; D2 plexus of canals)

BMC = bifid mandibular canal; MC = mandibular canal

Tab. II CT or CBCT studies evaluating the presence and morphology of BMCs

Author(s) and year	Country	N patients N sides (age)	Imaging technique	BMC classification	Mean frequency of BMCs	BMC subtypes	Comments
Naitoh et al. 2009	Japan	122 patients 244 sides (mean 50.8 years, 17–78 years)	CBCT	Naitoh	Patients: 64.8% Sides: 43.0%	Forward: 59.6% Retromolar: 29.8% Dental: 8.8% Buccolingual: 1.8%	–
Kuribayashi et al. 2010	Japan	252 patients 301 sides (mean 33 years, 18–74 years)	CBCT	Nortje	Sides: 15.6%	Type I: 4.3% Type II: 85.1% Type III: 0% Type IV: 10.6%	–
Naitoh et al. 2010	Japan	28 patients 56 sides (mean 54.5 years, 21–74 years)	CBCT	Naitoh	Sides: 32.1%	Forward: 84.2% Retromolar: 15.8% Dental: 0% Buccolingual: 0%	4 forward canals observed in CBCTs were not seen on CTs; 2 forward canals in CTs were longer than in CBCTs
		CTs were taken on average 30 months before CBCTs	Multislice CT		Sides: 25.0%	Forward: 80% Retromolar: 20% Dental: 0% Buccolingual: 0%	
Orhan et al. 2011	Turkey	242 patients 484 sides (mean 36.7 years, 17–83 years)	CBCT	Naitoh	Patients: 66.5% Sides: 46.5%	Forward: 38.2% Retromolar: 34.7% Buccolingual: 17.8% Dental: 9.3%	–
Yamada et al. 2011	Japan	96 patients 112 sides (mean NA, 16–77 years)	CBCT	Bifurcation from MC related to 3rd molar (M3)	(Sides: 94.6%)*	55.5% below M3 32.9% buccal to M3 11.6% lingual to M3	* Evaluation was limited to region of impacted lower 3rd molars (M3)
de Oliveira-Santos 2012	Belgium	100 patients 200 sides (age NA)	CBCT	–	Patients: 19%	Retromolar: 15.8% Forward: 10.5% Associated with double mental foramen: 31.6% Associated with accessory mental foramen: 42.1%	Only BMC with a diameter of >1mm included
Correr et al. 2013	Brazil	75 patients (unilateral exams) (mean 48.2 years, 17–83 years)	CBCT	Langlais	(Patients/sides: 100%)*	Type 1: 72.6% Type 2: 19.3% Type 3: 8% Type 4: 0%	* Selected cases with previously diagnosed BMC

BMC = bifid mandibular canal; CBCT = cone beam computed tomography; CT = computed tomography; MC = mandibular canal; NA = not available

Tab. II CT or CBCT studies evaluating the presence and morphology of BMCs continued

Author(s) and year	Country	N patients N sides (age)	Imaging technique	BMC classification	Mean frequency of BMCs	BMC subtypes	Comments
Choi & Han 2014	South Korea	446 patients 892 sides	CBCT	–	(Patients: 1.35% Sides: 0.9%)*	Retromolar canal: 75% Forward canal: 25%	* Evaluation was limited to canals originating from double mandibular foramina
Fu et al. 2014	Taiwan	173 patients 346 sides (mean 54 years, 14–85 years)	Multislice CT	–	Patients: 30.6% Sides: 18.5%	–	–
Kang et al. 2014	South Korea	1933 patients (unilateral exams) (mean 33 years, 13–93 years)	CBCT	Naitoh	Patients: 10.2%	Retromolar: 52.5% Forward: 40.9% Dental: 4.5% Buccolingual: 2%	–
Neves et al. 2014	Brazil	127 patients 254 sides (mean 41.9 years, 18–61 years)	CBCT	–	Patients: 9.8%	Canals located posterior to 3rd molar: 80% Canals located in mandibular body: 20%	Study also evaluated panoramic radiographs of same patients
Rashsuren et al. 2014	South Korea	500 patients 755 sides (age NA)	CBCT	Naitoh (modified)	Patients: 22.6% Sides: 16.2%	Retromolar: 71.3% Dental: 18.8% Forward: 4.1% Buccolingual: 0% Trifid: 5.8%	–
Shen et al. 2014	Taiwan	308 patients 616 sides (mean 51 years, 12–85 years)	135 CBCT	–	Patients: 41.2% Sides: 27.6%	–	–
			173 multislice CT				
Lima Villaca-Carvalho et al. 2016	Brazil	300 patients (mean NA, 25–87 years)	CBCT	–	Patients: 26.7%	–	–
Shen et al. 2016	Taiwan	327 patients 654 sides (mean 51 years, 23–85 years)	154 CBCT	–	Patients: 58.4% Sides: 42.2%	–	–
			173 multislice CT	–	Patients: 30.6% Sides: 18.7%	–	–
Afsa & Rahmati 2017	Iran	116 sides (age NA)	CBCT	–	Sides: 40.5%	–	–
Yang et al. 2017	China	280 patients 560 sides (mean 42 years, 18–78 years)	CBCT	Naitoh	Patients: 31.1%	Forward: 70.1% Retromolar: 15.9 Buccolingual: 12.1% Dental: 0% V type: 1.9%	V type = 2 branches arising from the MC, running forward and upward forming a V shape
de Castro et al. 2018	Canada	700 patients (mean 21.0 years, median 16 years)	CBCT	–	Patients: 41.1%	–	–

BMC = bifid mandibular canal; CBCT = cone beam computed tomography; CT = computed tomography; MC = mandibular canal; NA = not available

Tab. II CT or CBCT studies evaluating the presence and morphology of BMCs — continued

Author(s) and year	Country	N patients N sides (age)	Imaging technique	BMC classification	Mean frequency of BMCs	BMC subtypes	Comments
Shah et al. 2018	England	281 patients (unilateral exams) (mean 31.5 years, 14–79 years)	CBCT	Bifurcation from MC related to 3rd molar	Sides: 38%	Type 1 (ramus area): 57% Type 2 (area of 3rd molar): 38% Type 3 (area mesial to 3rd molar): 5%	For patients with bilateral images, one side was randomly selected for examination. Types refer to location of bifurcation.
Yoon et al. 2018	USA	194 patients 388 sides (mean 55 years, 13–103 years)	CBCT	Nortje	Patients: 13.4% Sides: 7.7%	Type I: 46.7% Type II: 53.3% Type III: 0% Type IV: 0%	–
Zhang et al. 2018	China	1000 patients 2000 sides (age NA)	CBCT	Naitoh	Patients: 13.2% Sides: 8.4%	Retromolar: 68.4% Dental: 14.9% Forward: 13.7% Buccolingual: 0% Trifid: 2.4% Bicanal: 0.6%*	* Bifurcates from inferior wall of MC
Luangchana et al. 2019	Thailand	176 patients 243 sides (mean 54.2 years, 20–86 years)	CBCT	Luangchana	Sides: 43.6%	Premolar/molar areas: Type A: 29%/32%/ Type B1: 0%/16% Type B2: 9%/13% Type C: 29%/39% Type D1: 19%/0% Type D2: 14%/0%	–
Okumus & Dumlu 2019	Turkey	500 patients 1000 sides (mean 38.2 years, 14–79 years)	CBCT	Naitoh	Patients: 40% Sides: 24.8%	Forward: 48.8% Retromolar: 26.2% Dental: 12.9% Buccolingual: 9.7% Trifid: 2.4%	–
Zhou et al. 2020	China	321 patients 642 sides (mean NA, range 8–80 years)	CBCT	Naitoh	Patients: 26.2% Sides: 16.4%	Forward: 40.0% Retromolar: 46.7% Dental: 10.5% Buccolingual: 2.9%	–

BMC = bifid mandibular canal; CBCT = cone beam computed tomography; CT = computed tomography; MC = mandibular canal; NA = not available

Tab. III Mean frequencies of BMCs per geographical regions

Geographical region	N studies[1]	Frequency per patients	Frequency per sides
Far East Asia (Japan, South Korea, China, Taiwan, Thailand)	12	10.2–64.8%	8.4–43.6%
Middle East Asia (Iran, Turkey)	3	40–66.5%	24.8–46.5%
Europe (Belgium, England)	2	19%[2]	38%[2]
Americas (USA, Canada, Brazil)	4	9.8–41.1%	7.7%[3]

BMC = bifid mandibular canal
[1] Three studies excluded for this analysis (Yamada et al. 2011, Correr et al. 2013, Choi & Han 2014) since study samples comprised only selected patients.
[2] Patient rate is lower than side rate, since the two reported values in this table are from two different studies.
[3] Data only from one study

Tab. IV Extension of BMCs (dental canals) to molars as reported using 3D radiography

Authors and year	N dental canals	Dental canal reaches 1st molar	Dental canal reaches 2nd molar	Dental canal reaches 3rd molar
Naitoh et al. 2011	10	–	20%	80%
Orhan et al. 2011	21	38%	5%	57%
Kang et al. 2014	9	–	–	100%
Zhang et al. 2018	25	–	16%	84%
Okumus & Dumlu 2019	32	47%	19%	34%

BMC = bifid mandibular canal

techniques: *in situ* (dry mandibles), panoramic radiography and 3D radiography (CT, CBCT) (Haas et al. 2016). The calculated mean frequencies were 6.5% *(in situ)*, 4.2% (panoramic radiography), and 16.3% (CT, CBCT). However, the included *in situ* studies were limited to the retromolar canals.

Several 3D radiography studies have assessed the frequency of BMCs (Tab. II). Data are either presented per patient or per hemimandible. The reported frequencies of BMCs per patient ranged from 9.8% to 66.5% and per mandibular side from 7.7% to 46.5%. A study limited to impacted 3rd molars even found a frequency of 94.6% of BMCs per side in that region (Yamada et al. 2011).

Some differences were noted for BMC detection rates when categorizing the results per geographical regions (Tab. III). Studies from Asia commonly reported higher BMC frequencies compared to studies from Europe or the Americas.

CT versus CBCT

Only one study has compared CT and CBCT of the same patients with regard to the radiographic identification of BMCs (Naitoh et al. 2010). The depiction rate per side was higher in CBCT (32.1%) than in CT (25.0%). However, no significant difference was reported. In another analysis by Shen et al. (2016), markedly higher BMC detection rates ($p < 0.001$) were reported for CBCT compared to CT (42.2% vs. 18.7% for hemimandibles and 58.4% vs. 30.6% for patients), but the two study samples were not identical.

Number of BMCs

Afsa & Rahmati (2017) reported mainly one BMC (31%) or two BMCs (6.9%) per evaluated side; however, in one patient, they found five BMCs on one side.

Influence of gender, age, or side

With regard to gender, Fu et al. (2014) found significantly more BMCs (per hemimandible) in males (26.7%, $p = 0.028$) compared to females (14.4%). Also, Luangchana et al. (2019) reported significantly more BMCs (per hemimandible) in males (52.5%, $p = 0.020$) than in females (37.5%). However, the majority of studies reported no significant gender difference for BMC frequency (Kang et al. 2014; Rashsuren et al. 2014; Lima et al. 2016; Yoon et al. 2018; Zhang et al. 2018; Okumus & Dumlu 2019; Zhou et al. 2020).

Regarding age, patients ≤20 years of age had a significantly lower BMC frequency (4.2%, $p < 0.05$) compared to other age groups (15.2–22.8%) (Zhang et al. 2018). Similarly, Okumus & Dumlu (2019) noted a significantly lower BMC frequency (14.5%, $p = 0.006$) in subjects younger than 25 years of age compared to older age groups (26.5–30.5%). In contrast, Rashsuren et al. (2014) as well as Kang et al. (2014) reported no significant differences for BMC frequency among various age groups. Yoon et al. (2018) stated that ethnicity was not a significant predictor for BMC prevalence.

Studies comparing right and left hemimandibles found no difference for side predilection of BMCs (Lima et al. 2016; Luangchana et al. 2019; Zhou et al. 2020).

Tab. V Confluence of BMCs (forward canals) as reported using 3D radiography

Authors and year	N forward canals	Confluence of forward canal with MC
Naitoh et al. 2011	68	7.4%
Orhan et al. 2011	86	31.4%
Kang et al. 2014	81	11.1%
Zhang et al. 2018	23	43.5%
Okumus & Dumlu 2019	121	15.7%

BMC = bifid mandibular canal

Location of BMC origin

According to Shen et al. (2014), 27.7% of BMCs originated in the ramus, 40% in the retromolar area, 17.1% in the molar region, 11.8% in the premolar region, and 3.5% anterior to the mental foramen. Afsa & Rahmati (2017) described 25.4% of BMCs bifurcating in the ramus, also 25.4% in the retromolar area, and 49.2% in the molar region. Yang et al. (2017) reported in 38.3% a BMC origin in the ramus, in 27.1% in the retromolar region, and in 34.6% in the molar area.

Distance from mandibular foramen to BMC bifurcation

Zhang et al. (2018) measured a mean distance of 8.1 ± 5.6 mm from the mandibular foramen to the BMC origin. No significant differences were noted among the various BMC subtypes.

Course of BMCs

Several authors provided details with regard to dental canals and their extensions to adjacent root apices (Tab. IV). Overall, the majority of dental canals reached the 3rd molars. Regarding the so-called forward canals, some of these BMCs rejoined the main canal anteriorly with confluence rates of 7.4 to 43.5% (Tab. V).

Tab. VI Mean length (mm) of BMCs as reported using 3D radiography

Authors and year	N BMCs	All BMCs	Retromolar canals	Dental canals	Forward canals	Buccolingual canals	Comments
Naitoh et al. 2009	114	–	14.8[1,2,3] (7.2–24.5)	8.9[1] (1.6–23)	9.6[2,4] (1.4–25)	1.6[3,4] (1.5–1.7)	Same superscripts denote statistically significant differences
Orhan et al. 2011	225	13.6 (right sides) 14.1 (left sides)	13.5	8.3	20.1	3.8	–
Fu et al. 2014	64	10.2 ± 4.8 (3.5–24.3)	–	–	–	–	Males: 11.5 ± 5.7 Females: 8.2 ± 2.4 (statistically significant difference)
Kang et al. 2014	198	15.0 (2.2–38.8)	16.2[1] (2.2–33.2)	8.7[1,2,3] (3.1–20.9)	14.0[2] (2.6–38.8)	16.0[3] (9.4–22.3)	Same superscripts denote statistically significant differences
Rashsuren et al. 2014	122	16.9 ± 6.8	17.9 ± 6.7	10.7 ± 3.01	18.9 ± 9.3	–	Trifid canals (n = 7): 20.1 ± 5.81
Afsa & Rahmati 2017	63	13.6 (3.9–48.5)	10.5 (4.1–20)	13.6 (4.9–26.2)	–	–	Ramus canals: 16.9 (3.9–48.5)
Zhang et al. 2018	168	12.6 ± 4.9	13.3 ± 4.4[1]	10.3 ± 5.3[1,2]	12.2 ± 5.9[2]	–	Same superscripts denote statistically significant differences
Zhou et al. 2020	105	13.7* (2.6–28.8)	–	–	–	–	* Median value Gender did not influence BMC length

BMC = bifid mandibular canal; CBCT = cone beam computed tomography; CT = computed tomography; MC = mandibular canal; NA = not available

Tab. VII Mean diameter (mm) of BMCs as reported using 3D radiography

Authors and year	N BMCs	All BMCs	Retromolar canals	Dental canals	Forward canals	Buccolingual canals	Comments
Kuribayashi et al. 2010	47	1.68 (0.88–3.4)	–	–	–	–	Diameter ≥50% of main canal: 49% Diameter <50% of main canal: 51%
de Oliveira et al. 2012	NA	1.5 ± 0.2 (1.03–3.3)	–	–	–	–	Diameter measured at widest portion of BMC
Fu et al. 2014	64	0.9 ± 0.4 (0.4–2.1)	–	–	–	–	Gender or side did not influence BMC diameter
Kang et al. 2014	198	1.27 (0.27–3.29)	1.36 (0.27–3.29)	0.91 (0.64–1.29)	1.21 (0.59–3.0)	1.14 (0.95–1.33)	No statistically significant differences among canal types
Rashsuren et al. 2014	122	2.2 ± 0.5	2.2 ± 0.5	2.1 ± 0.4	1.9 ± 0.3	–	Trifid canals (n = 7): 2.0 ± 0.4 Diameter measured at widest portion of BMC
Afsa & Rahmati 2017	63	1.12 (0.4–3.6)	1.02 (0.4–1.8)	1.0[1] (0.4–1.8)	–	–	Ramus canals: 1.42[1] (0.7–3.6) Same superscripts denote statistically significant difference
Shah et al. 2018	113	–	–	–	–	–	Diameter ≥50% of main canal: 23% Diameter <50% of main canal: 77%
Zhang et al. 2018	168	2.1 ± 1.4	2.28[1,2] ± 1.29	1.75[1] ±0.53	1.74[2] ±0.68	–	Same superscripts denote statistically significant differences
Zhou et al. 2020	105	2.26* (1.24–5.55)	–	–	–	–	* Median value Gender did not influence BMC diameter

BMC = bifid mandibular canal; CBCT = cone beam computed tomography; CT = computed tomography; MC = mandibular canal; NA = not available

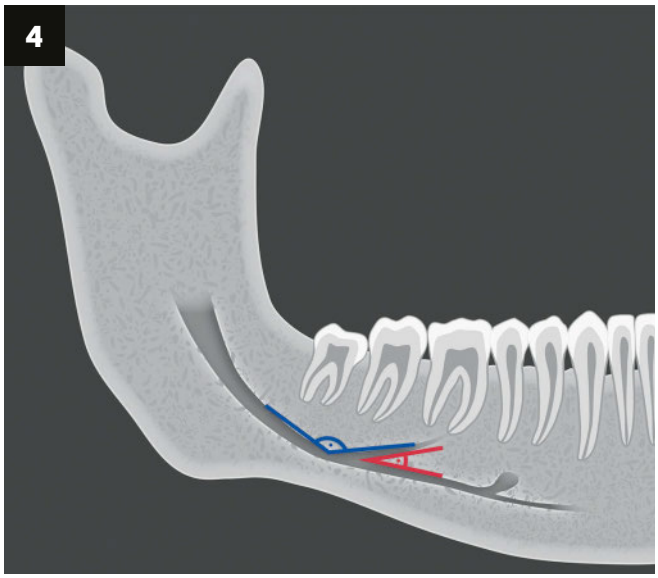

Fig. 4 Schematic illustration demonstrating superior and inferior angles of bifurcation of BMC from MC.

Orhan et al. (2011) identified 40 buccolingual BMCs (23 buccal, 17 lingual). All were located in the ramus region. Shen et al. (2014) detected 170 BMCs of which 95.9% originated from the superior MC wall. In 16.5% of identified BMCs, an accessory foramen was formed in the mandibular cortex by the accessory canal.

Shah et al. (2018) assessed the direction of BMCs in the vicinity of 3rd molars. The majority had a superior (65%) or superolateral (27%) course; only one BMC (1%) showed an inferior direction. The remaining BMCs ran either buccally or lingually to the main canal. Zhang et al. (2018) described a BMC originating from the lower part of the mandibular foramen, coursing antero-inferiorly, and terminating at a foramen on the lingual cortex of the ramus.

Length of BMCs

Several research groups assessed the mean length of BMCs overall and per canal type (Tab. VI). For all canals, the pooled mean lengths ranged from 10.2 to 16.9 mm. Marked differences of canal length were described for the various BMC types. The shortest mean length was 1.6 mm for buccolingual canals, and the longest mean length was 20.1 mm for forward canals.

Diameter of BMCs

The mean diameter of BMCs ranged between 0.9 and 2.3 mm (Tab. VII). Some authors also assessed the diameter of the main canal with mean values of 2.9 to 5.0 mm (Kuribayashi et al. 2010; Kang et al. 2014; Rashsuren et al. 2014; Zhou et al. 2020). While Kang et al. (2014) found no significant differences for mean canal diameters among the various BMC types, other authors reported significant differences (Afsa & Rahmati 2017; Zhang et al. 2018).

Angle of BMCs

Some radiographic studies have assessed the inferior and/or superior angles of bifurcation of BMCs from the main canal (Fig. 4). Orhan et al. (2011) reported mean angles for right and left sides of 139° and 141° for superior angles, and of 38° and 32° for inferior angles. Side and gender had no significant influence on the calculated values. Rashsuren et al. (2014) observed a mean angle of 149.2° ± 22.7° for superior angles and 37.7° ± 24.1° for inferior angles. Superior angles did not significantly differ among the various canal types. However, retromolar canals had a significantly greater mean inferior angle (44.1° ± 26.1°) than dental (24.6° ± 11.7°, $p < 0.05$) or trifid canals (25.2° ± 10.1°, $p < 0.05$). Also, Zhang et al. (2018) reported significant differences for mean inferior angles comparing the various BMCs: 52.4° for retromolar canals, 23.8° for dental canals, and 2.4° for forward canals.

Distance from BMCs to root apices

Yoon et al. (2018) measured the greatest distance between the superior border of a BMC and the apex of the closest root when applicable. The average distance was 3.45 mm on left sides and 4.85 mm on right sides.

Corticalization of BMCs

One research group published two papers addressing the corticalization of BMCs (Shen et al. 2014, 2016). In the first study, Shen et al. (2014) calculated the degree of corticalization of 170 BMCs using either multislice CT or CBCT. Degree of corticalization was complete (>85%) in 44.7%, moderate (50–84%) in 23.5%, mild (16–49%) in 10%, and minimal/none (<15%) in 21.8% of the assessed BMCs.

In the second study by Shen et al. (2016) including 194 BMCs, figures of corticalization degree were similar to those mentioned above (40.7%, 23.7%, 12.4%, 23.2%). In addition, the authors reported a mean thickness of BMC corticalization of 0.48 mm in CBCT and 0.65 mm in CT ($p < 0.001$). Cortex thickness of BMCs and degree of corticalization were significantly correlated ($R^2 = 0.530$, $p < 0.001$).

Discussion

This literature review collected and presented morphological and quantitative data of BMCs as identified by means of 3D radiography. The fact that studies using CT and/or CBCT have reported higher rates of BMCs compared to those using panoramic radiography is comprehensible. Zhang et al. (2018) assessed concomitant panoramic radiographs of patients with BMCs detected in CBCT. Only 7.1% of BMCs were visible in panoramic views. The authors concluded that the latter is an unreliable imaging method for the detection of BMCs. Similarly, Shah et al. (2018) demonstrated that the sensitivity of panoramic radiography to identify BMCs was poor (11%).

However, for cost and radiation issues, CBCT should not be used routinely for planning dental or surgical interventions in the mandible. Nevertheless, the limitations of panoramic views are known, and caution must be exercised when relying on the assessment of variations of the mandibular canal based on two-dimensional radiography alone (Haas et al. 2016; Zhang et al. 2018). Therefore, when in doubt, CBCT is suggested for a detailed, three-dimensional evaluation and identification of potential bifid mandibular canals before surgical procedures to avoid perioperative complications (de Castro et al. 2018; Zhou et al. 2020). Furthermore, in case a CBCT has already been taken, the clinician is advised to carefully search for the presence of a BMC to avoid adverse effects.

The great discrepancy of BMC occurrences among the assessed CBCT studies is surprising (Tab. II). According to Zhang et al. (2018), these variations of results may be explained by the following factors:

Tab. VIII New classification of BMC (L–Or–Di–Co–T) based on 3D radiography

	Location **Site where BMC arises**	**Or**igin **Structure from which BMC arises**	**Di**rection **Course of BMC**	**Co**nfiguration **Morphology of BMC**	**T**ermination **End of BMC**
1	Ramus	Duplicate mandibular foramen	Superior	Single canal	Joins root apex
2	Retromolar/3rd molar area	Mandibular canal	Anterior	Branching canal	Rejoins mandibular canal
3	Region of 2nd molar to mental foramen	Other BMC	Inferior	Multiple canals or plexus	Rejoins other BMC
4	Zone anterior to mental foramen	Other structure	Posterior		Buccal or lingual cortical foramen
5			Lateral		Retromolar foramen
6			Medial		Vanishes in bone

BMC = bifid mandibular canal

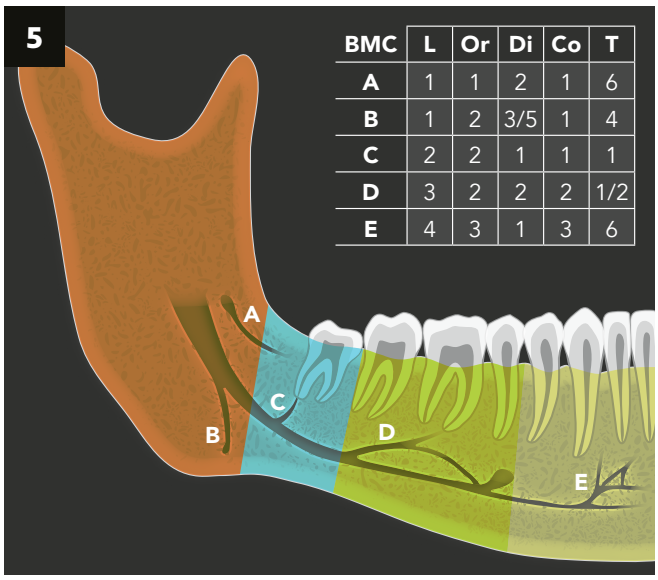

Fig. 5 Schematic illustration of new BMC classification based on **L–Or–Di–Co–T** (see also Tab. VIII).

- Different study populations: ethnicity, sample size, patient characteristics
- Imaging technique issues: resolution, voxel size, field of view, quality of images (artefacts, motion, noise)
- Radiographic assessment: experience of observer, criteria of BMC definition, interpretation of anatomical structures

Historically, BMCs have been described and categorized using panoramic radiographs (Nortje et al. 1977; Langlais et al. 1985) (Tab. I). However, due to the inherent limitations of two-dimensional radiography for correct representation of anatomical structures, such classifications should no longer be used. Newer classifications based on CBCT imaging (Naitoh et al. 2009; Luangchana et al. 2009) are more accurate but still do not cover all possible BMC variations. In this context, Shen et al. (2014) reported that 38% of detected BMCs did not fit into the classification of Naitoh et al. (2009). In addition to the four BMC types categorized by Naitoh et al. (2009), a so-called V-type canal was described by Yang et al. (2017), and trifid canals were reported by Okumus & Dumlu (2019) (Tab. II). Therefore, we suggest a new BMC classification based on five parameters: i.e., location, origin, direction, configuration and termination (Tab. VIII and Fig. 5).

Failure to accurately locate a BMC may result in damage to the canal with subsequent complications including traumatic neuroma, sensory disturbances, intra- or postoperative bleeding and hematoma formation (Shah et al. 2018; Zhang et al. 2018). Case reports have documented severe and persistent pain following implant placement in the posterior mandible despite optimal anatomical host sites in panoramic radiography (Maqbool et al. 2013; Aljunid et al. 2016). However, subsequent CBCT imaging demonstrated that the implants impinged on BMCs. After the removal of those implants breaching the accessory canals, significant pain reduction was observed (Fig. 6).

A severe bleeding complication related to a BMC was reported by Verea Linares et al. (2016). A partially erupted 3rd molar closely associated with a BMC was treated with coronectomy. The patient subsequently needed emergency hemorrhage control under general anesthesia due to failure of local measures to arrest bleeding. The authors suggested cross-sectional imaging for adequate surgery planning when a BMC is suspected. Furthermore, they recommended complete removal of the tooth instead of coronectomy to enable direct access to the bleeding source (Fig. 7).

Other clinically relevant complications include overinstrumentation and/or extrusion of filling materials during endodontic treatment. The latter may injure the neurovascular structures of the MC directly or indirectly via a BMC (Fig. 8). This will result in severe complications including throbbing pain, alterations or loss of sensitivity, and/or necrosis of skin or mucosa (Nicolau syndrome) (Lindgren et al. 2002; Sharma et al. 2008; Wilbrand et al. 2011).

The presence of BMCs may also be associated with increased difficulty in obtaining mandibular anesthesia with a conventional block of the inferior alveolar nerve (IAN) (Lew & Townsend 2006). This would be most likely the case when an accessory canal originates from a duplicate foramen, often located superior to the mandibular foramen. To overcome this problem, it was suggested to apply the Gow-Gates or Akinosi-Varizani tech-

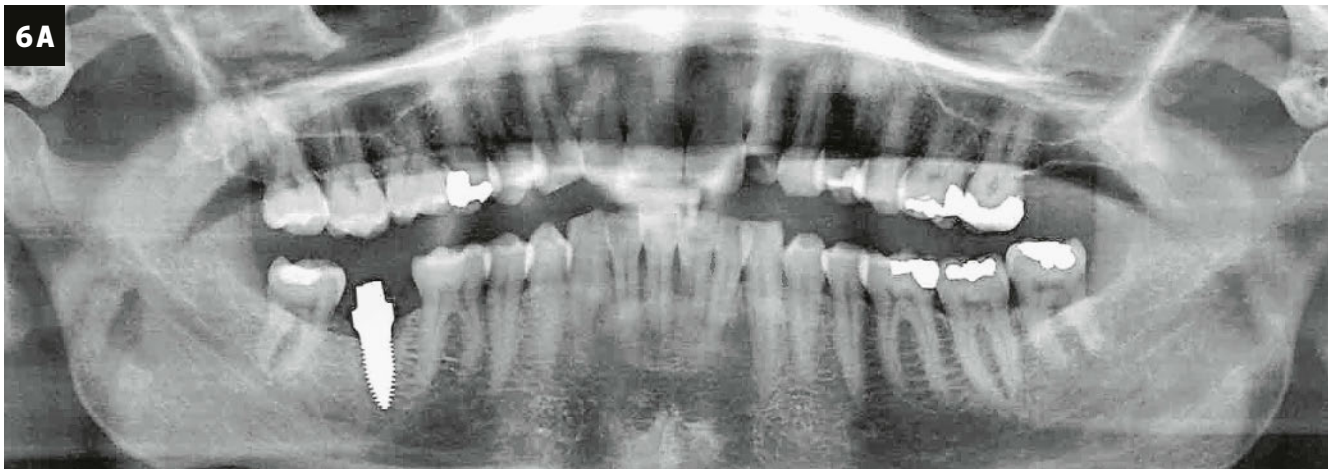

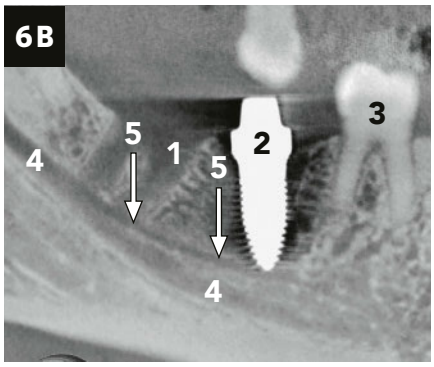

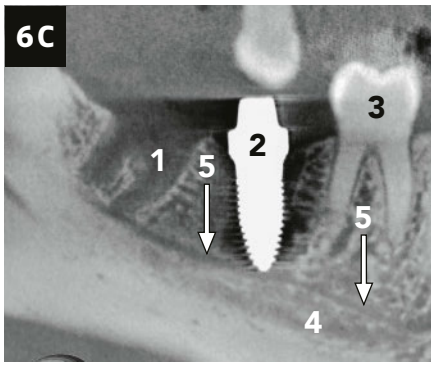

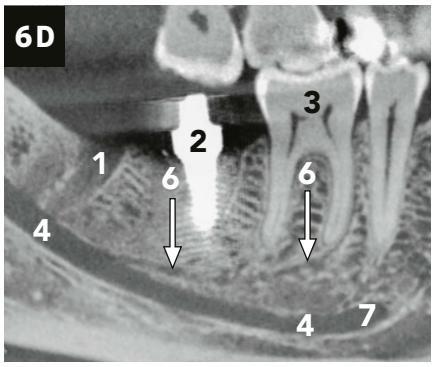

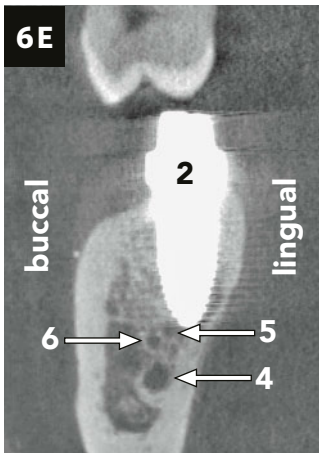

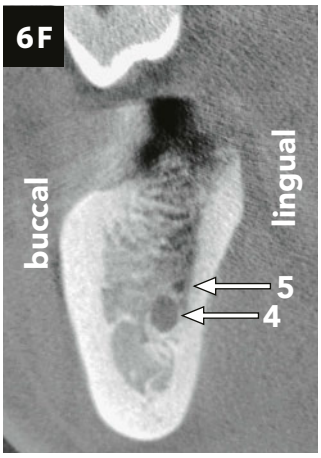

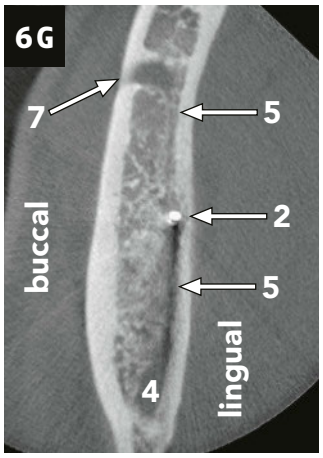

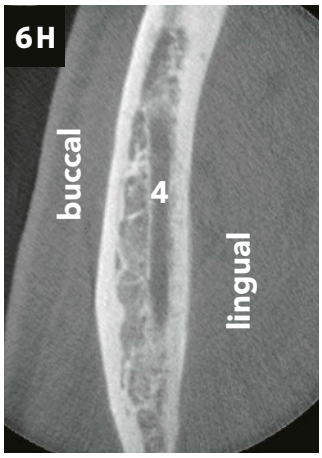

Fig. 6 Referral of a 47-year-old female with severe pain and sensitivity loss in the right lower lip and chin areas following implant insertion in the position of the lower right second molar (47). Panoramic radiograph by private dentist shows good distance from implant tip to mandibular canal (A); tooth 48 was subsequently removed by the referring dentist hoping that the sensitivity would improve but it didn't. CBCT images show that the implant is impinging on a BMC that rejoins the MC. An additional BMC to the mesial root of tooth 46 is visible. Sagittal images (B, C, D), coronal image (E, F), and axial images (G, H, all inferior view). A 3D illustration demonstrates the BMC courses (I): for **L–Or–Di–Co–T** numbers, refer to Table VIII.
1 = socket of extracted 48; 2 = implant for replacement of tooth 47; 3 = tooth 46; 4 = MC; 5 = BMC rejoining MC; 6 = BMC extending to mesial root of 46; 7 = mental foramen.

6I

BMC	L	Or	Di	Co	T
5	2	2	2/3	1	2
6	3	2	2	1	1

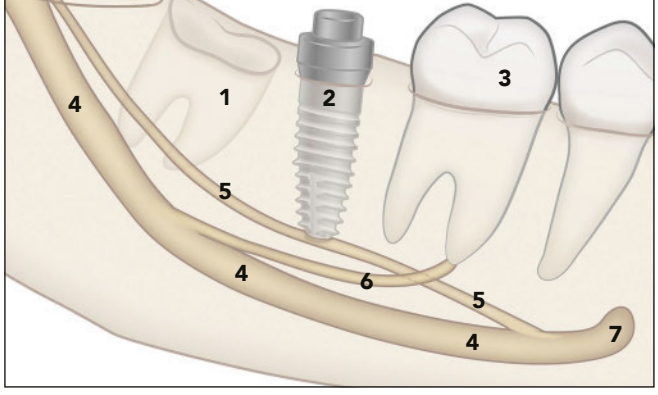

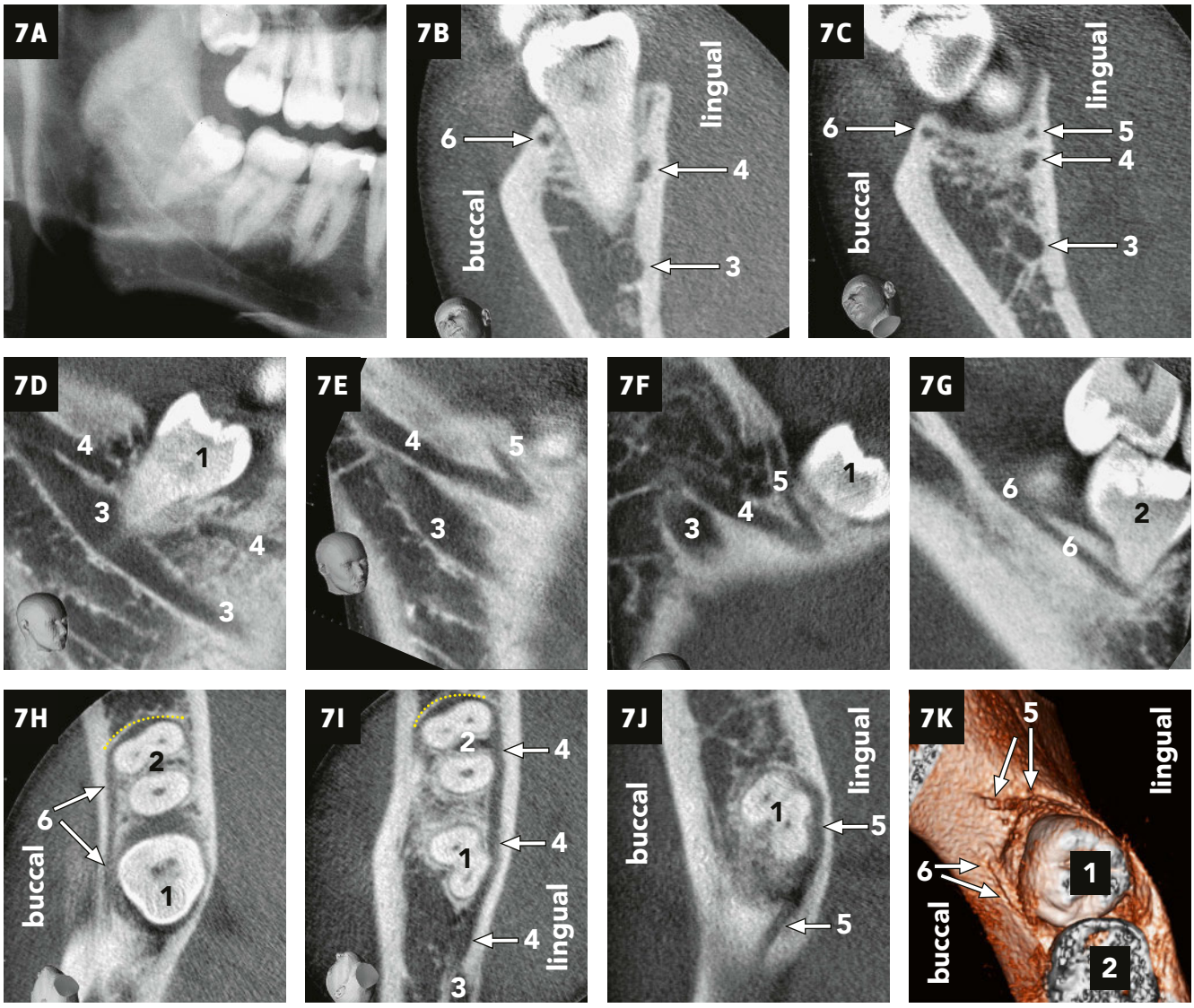

7L

BMC	L	Or	Di	Co	T
4	2	2	2	1	3
5	2	3	1	1	5
6	3	3	4/5	1	4

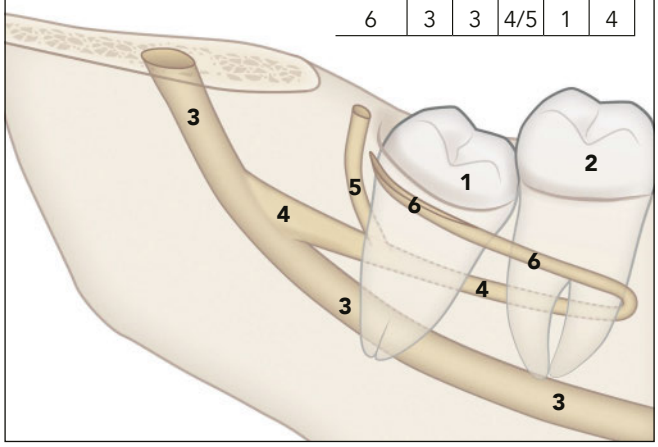

Fig. 7 Radiographic assessment of a lower right 3rd molar (48) in a 32-year-old male. A BMC is assumed on the cropped panoramic radiograph (A), but in fact, three BMCs are visible on the CBCT images. Sagittal images (D, E, F, G), coronal images (B, C), axial images (H, I, J, all inferior view), and 3D-rendered image (K, superior view). A 3D illustration demonstrates the complex BMC courses (L): for **L-Or-Di-Co-T** numbers, refer to Table VIII.
1 = tooth 48; 2 = tooth 47; 3 = MC; 4 = large lingual BMC; 5 = branching upper lingual BMC; 6 = small buccal BMC. Dotted yellow line (in H and I) represents fusion of large lingual and small buccal BMCs.

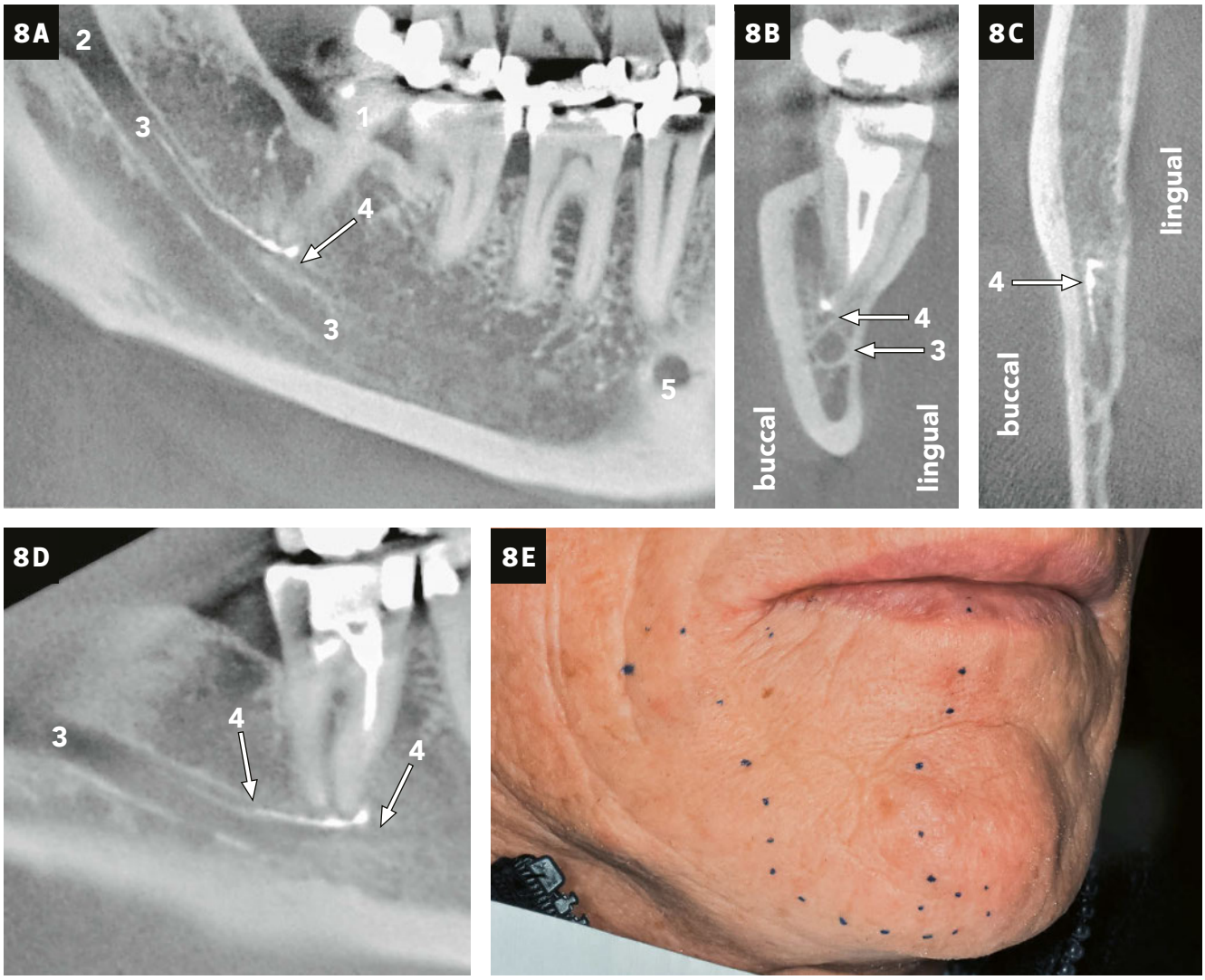

Fig. 8 CBCT assessment of a 62-year-old male presenting severe pain and sensitivity loss following root canal medication with calcium hydroxide ($CaOH_2$) of the lower right 3rd molar (tooth 48). The CBCT images clearly exhibit overfilling and migration of $CaOH_2$ in a BMC running below 48. Sagittal images (A, D), coronal image (B), axial image (C, inferior view), and clinical picture showing the extent of the sensitivity loss (E).
1 = tooth 48; 2 = mandibular foramen; 3 = MC; 4 = BMC with overfilled $CaOH_2$; 5 = mental foramen.

niques for "high" IAN blocks (Lew & Townsend 2006; Okumus & Dumlu 2019).

Commonly, the BMC is considered a duplication or division of the MC. BMCs were also described as tubular bony structures branching from the MC (Yamada et al. 2011). However, radiographically it is not possible to know whether these tubular bony structures contain branches from the inferior alveolar nerve and/or artery. A histologic analysis of the neurovascular content of the BMC has so far only been done with regard to retromolar canals, but not with regard to forward canals (von Arx et al. 2011; Fukami et al. 2012).

Radiographic interpretation of tubular bony structures is a challenge, even with 3D-imaging techniques. Superimposition of other anatomical structures, i.e., the mylohyoid groove or canal, as well as the internal oblique line that serves for the attachment of the mylohyoid muscle, may result in misdiagnosis, in particular with panoramic radiography (Auluck & Pai 2005; Serman 2012; Neves et al. 2014). Dense trabecular structures may also give the illusion of a BMC in radiographs. Kim et al. (2011) documented a dry mandible with radiographic suspicion of a BMC (panoramic radiography, CBCT, micro CT). However, stereoscopic and histologic examinations of cross-sections showed that only the superior canal (round shape) contained neurovascular bundles while the inferior canal (elliptical shape) contained marrow tissue. In the future, high resolution MRI with identification of blood vessels and nerves might be a hopeful and promising step for enhanced diagnosis of BMCs (Krasny et al. 2012a, 2012b).

In conclusion, the presence of a BMC must be taken into consideration in dental medicine, and specifically for treatment planning and anesthetic, endodontic, or surgical interventions in the posterior mandible. Any situation with inexplicable sensitivity disturbances or hemorrhage/hematoma formation in the mandible might be associated with a (radiographically invisible) BMC containing neurovascular structures. The clinician is then advised to obtain a 3D image, preferably a CBCT.

Acknowledgement

The authors thank Bernadette Rawyler, Medical Illustrator, and Ines Badertscher, Media Designer, School of Dental Medicine, University of Bern, Bern, Switzerland, for the illustrations and the preparation of the figures.

Zusammenfassung

Der Mandibularkanal ist eine prominente anatomische Struktur im Unterkiefer. Wegen seines neurovaskulären Inhaltes hat der Mandibularkanal grosse klinische Bedeutung. Eine Schädigung des Mandibularkanals kann zu schwerwiegenden Sensibilitätsstörungen oder Blutungskomplikationen führen. Die embryologische Entwicklung des Mandibularkanals ist streng mit der neurovaskulären Versorgung der pränatalen Zahnanlagen verbunden. Eine einmalige Studie von 302 Unterkieferhälften von Foeten zeigte, dass sich zuerst ein Kanal zu den Milchinzisiven bildet, dann zu den Milchmolaren und später auch zu den bleibenden Molaren. In der Regel kommt es dann in der Weiterentwicklung des Unterkiefers zur Fusion dieser drei Kanäle zu einem Mandibularkanal. Bei fehlender oder unregelmässiger Verschmelzung kommt es jedoch zu anatomischen Variationen wie *Canalis bifidus* (oder *trifidus*) *mandibulae.*

Ziel dieser Literaturübersicht ist die Präsentation von morphologischen und quantitativen Daten basierend auf 3-D-Röntgen bezüglich des *Canalis bifidus.* Dazu erfolgte eine Literatursuche in «PubMed» (www.ncbi.nlm.nih.gov/pubmed) bezüglich relevanter radiologischer Studien. Ausgenommen wurden Arbeiten, die sich ausschliesslich mit dem Retromolarkanal befassten. Auch Studien, die rein auf Panoramaschichtaufnahmen basierten, wurden ausgeschlossen.

Die Angaben in den analysierten Studien bezüglich der Häufigkeiten des *Canalis bifidus* variieren stark: 9,8–66,5% pro Patient und 7,7–46.5% pro Unterkieferseiten. Gründe können unterschiedliche Studienpopulationen sein, Limitationen in der Bildgebung oder Schwierigkeiten bei der Interpretation anatomischer Strukturen. Die meisten Studien berichteten über keine Unterschiede in den Häufigkeiten bei Männern und Frauen. Einzelne Arbeiten fanden eine statistisch signifikant geringere Häufigkeit des *Canalis bifidus* bis 20 bzw. 25 Jahre im Vergleich zu den älteren Patientengruppen.

Ein *Canalis bifidus* kann im gesamten Unterkiefer beobachtet werden, also vom Ramus bis zur Region anterior des *Foramen mentale.* Morphologische Variationen und Kanalverläufe sind äusserst vielfältig. Ausgangspunkt des *Canalis bifidus* ist in der Regel der Mandibularkanal, seltener ein akzessorisches Foramen im Ramus oder in der Retromolarregion. Die Kanäle ziehen dann meistens nach oben zur Retromolarregion, schräg nach oben zu den Wurzelspitzen der Molaren oder horizontal nach vorne unterhalb der Wurzelspitzen der (Prä-)Molaren. Letztere Kanäle verschmelzen in 7,4–43,5% wieder mit dem Mandibularkanal.

Quantitative Daten ergeben für den *Canalis bifidus* durchschnittliche Längen von 10,2 bis 16,9 mm und Durchmesser von 0,9 bis 2,2 mm. Einzelne Autoren haben auch die durchschnittlichen Bifurkationswinkel beim Abgang des *Canalis bifidus* vom Mandibularkanal gemessen (139–149° für den oberen Winkel und 32–38° für den unteren Winkel). Zwei Studien haben den Grad der Kortikalisierung des *Canalis bifidus* untersucht. Dabei zeigten beide Studien eine maximale Kortikalisierung in 45% bzw. 41% als häufigste Resultate.

Historisch erfolgte die Einteilung des *Canalis bifidus* auf den Klassifikationen von Nortje et al. (1977) sowie Langlais et al. (1985), die aber beide auf Panoramaschichtaufnahmen basierten. Erst über 20 Jahre später erschien dann eine neue und auf der digitalen Volumentomografie abstützende Einteilung durch Naitoh et al. (2009). Wegen der äusserst vielseitigen Variationen des *Canalis bifidus* erlaubt aber auch diese Klassifikation keine abschliessende Einteilung aller akzessorischer Kanäle. Wir schlagen deshalb eine umfassende Klassifikation des *Canalis bifidus* vor, die auf fünf Parameter beruht: Lokalisation, Ursprung, Richtung, Konfiguration und Ende des *Canalis bifidus.*

In der Literatur finden sich im Zusammenhang mit einem *Canalis bifidus* Hinweise für Schwierigkeiten bei der Leitungsanästhesie, Komplikationen nach endodontologischer oder implantologischer Therapie sowie schwere Nachblutungen nach Weisheitszahnentfernung. Als Schlussfolgerung muss die Möglichkeit eines *Canalis bifidus* für die Planung und Durchführung von Anästhesien, Wurzelkanalbehandlungen sowie chirurgischen Eingriffen im Unterkiefer unbedingt berücksichtig werden.

Résumé

Le canal mandibulaire est une structure anatomique proéminente de la mâchoire inférieure. Il a une grande importance clinique, car il conduit entre autres le pédicule alvéolaire inférieur. Un dommage au canal mandibulaire peut provoquer de sérieux troubles de la sensibilité ou des hémorrhagies. Le développement embryologique du canal mandibulaire est lié à l'alimentation neuro-vasculaire prénatale des germes dentaires. Une étude exceptionnelle de 302 hémi-mandibules de fœtus a montré qu'un premier canal se forme vers les incisives de lait, un deuxième vers les molaires de lait, et un troisième vers les molaires permanentes. En règle générale, ces trois canaux fusionnent et forment le canal mandibulaire lors du développement ultérieur de la mâchoire inférieure. Les variations anatomiques du *Canalis bifidus* (ou *trifidus*) *mandibulae* surviennent lors de fusion incomplète ou manquante.

Le but de cet aperçu de la littérature est la présentation des données morphologiques et quantitatives du *Canalis bifidus* visualisé sur des radiographies tridimensionnelles. Pour cela, une recherche de la littérature a été réalisée sur « PubMed » (www.ncbi.nlm.nih.gov/pubmed) en quête d'études radiologiques pertinentes. Les études qui n'analysent que le canal rétro-molaire ont été exclues. Les études qui n'analysent que les radiographies panoramiques ont également été exclues.

L'incidence du *Canalis bifidus* varie fortement selon les études analysées : 9,8–66,5 % des patients et 7,7–46,5 % des hémi-mandibules. Cela peut être expliqué par les différentes populations analysées, les limitations des radiographies, et les difficultés d'interprétation des structures anatomiques. La plupart des études n'ont pas trouvé de différence d'incidence entre les hommes et les femmes. Quelques études ont montré un abaissement de l'incidence statistiquement significatif du *Canalis bifidus* chez les personnes jusqu'à l'âge de 20 ou respectivement 25 ans en comparaison aux patients plus âgés.

Un *Canalis bifidus* peut être visible sur toute la longueur de la mandibule, c'est-à-dire de la branche mandibulaire au foramen mentonnier. La morphologie et l'orientation des canaux sont extrêmement variables. L'origine du *Canalis bifidus* est en règle générale le canal mandibulaire, moins fréquemment un foramen supplémentaire dans la branche mandibulaire ou dans la région rétro-molaire. La plupart des canaux montrent un cheminement vers le haut, vers la région rétro-molaire, courent obliquement en direction des pointes des racines des molaires, ou se dirigent horizontalement vers l'avant sous les racines des (pré)molaires. Ces derniers montrent dans 7,4–43,5 % des cas une confluence avec le canal mandibulaire.

Les données quantitatives concernent la longueur moyenne (10,2–16,9 mm) et le diamètre moyen (0,9–2,2 mm) du *Canalis bifidus.* Quelques auteurs mesurent aussi les angles de bifur-

cation à l'origine du *Canalis bifidus* du canal mandibulaire (139–149° pour l'angle supérieur et 32–38° pour l'angle inférieur). Deux études évaluent le degré de corticalisation du *Canalis bifidus* et montrent le plus fréquemment une corticalisation maximale de 45 %, respectivement 41 %.

Historiquement, la classification du *Canalis bifidus* a été faite par Nortje et al. (1977) et Langlais et al. (1985), qui se basaient les deux sur des radiographies panoramiques. 20 ans plus tard, une nouvelle classification a été proposée par Naitoh et al. (2009), cette fois basée sur la tomographie volumétrique numérisée. Mais même cette classification ne permet pas une différentiation complète des canaux supplémentaires en raison de variations multiples. Nous proposons donc une classification différentiée du *Canalis bifidus* selon cinq paramètres : localisation, origine, direction, configuration et terminaison du *Canalis bifidus*.

Dans la littérature, on trouve une corrélation entre le *Canalis bifidus* et des difficultés lors d'anesthésies tronculaires, des complications après des interventions endodontiques ou implantaires, ainsi que des saignements sérieux après l'ostéotomie des dents de sagesse. En conclusion, il faut tenir compte d'un possible *Canalis bifidus* lors de la planification et de l'exécution des anesthésies, des traitements de racine, ainsi que des interventions chirurgicales dans la mandibule.

References

Afsa M, Rahmati H: Branching of mandibular canal on cone beam computed tomography. Singapore Dent J 38: 21–25 (2017)

Aljunid S, AlSiweedi S, Nambiar P, Chai W L, Ngeow W C: The management of persistent pain from a branch of the trifid mandibular canal due to implant impingement. J Oral Implantol 42: 349–352 (2016)

Angelopoulos C, Thomas S, Hechler S, Parissis N, Hlavacek M: Comparison between digital panoramic radiography and cone beam computed tomography for the identification of the mandibular canal as part of presurgical dental implant assessment. J Oral Maxillofac Surg 66: 2130–2135 (2008)

Auluck A, Pai K M: Letter to the editor. Trifid mandibular canal. Dentomaxillofac Radiol 34: 259 (2005)

Bürklein S, Grund C, Schäfer E: Relationship between root apices and the mandibular canal: A cone-beam computed tomographic analysis in a German population. J Endod 41: 1696–1700 (2015)

Carter R B, Keen E N: The intramandibular course of the inferior alveolar nerve. J Anat 108: 433–440 (1971)

Castro M A A, Lagravere-Vich M O, Amaral T M P, Abreu M H G, Mesquita R A: Classifications of mandibular canal branching: A review of literature. World J Radiol 28: 531–537 (2015)

Chavez-Lomeli M E, Lory J M, Pompa J A, Kjaer I: The human mandibular canal arises from three separate canals innervating different tooth groups. J Dent Res 75: 1540–1544 (1996)

Choi Y Y, Han S S: Double mandibular foramen leading to the accessory canal on the mandibular ramus. Surg Radiol Anat 36: 851–855 (2014)

Correr G M, Iwanko D, Leonardi D P, Ulbrich L M, de Araujo M R, Deliberador T M: Classification of bifid mandibular canals using cone beam computed tomography. Braz Oral Res 27: 510–516 (2013)

de Castro M A, Barra S G, Lagravere Vich M O, Abreu Mhg, Mesquita R A: Mandibular canal branching assessed with cone beam computed tomography. Radiol Med 123: 601–608 (2018)

de Oliveira-Santos C, Souza P H, de Azambuja Berti-Couto S, Stinkens L, Moyaert K, Fischer Rubira-Bullen I R, Jacobs R: Assessment of variations of the mandibular canal through cone beam computed tomography. Clin Oral Invest 16: 387–393 (2012)

Fu E, Peng M, Chiang C Y, Tu H P, Lin Y S, Shen E C: Bifid mandibular canals and the factors associated with their presence: A medical computed tomography evaluation in a Taiwanese population. Clin Oral Impl Res 25: e64–67 (2014)

Fukami K, Shiozaki K, Mishima A, Kuribayashi A, Hamada Y, Kobayashi K: Bifid mandibular canal: Confirmation of limited cone beam CT findings by gross anatomical and histological investigations. Dentomaxillofac Radiol 41: 460–465 (2012)

Haas L F, Dutra K, Porporatti A L, Mezzomo L A, de Luca Canto G, Flores-Mir C, Correa M: Anatomical variations of mandibular canal detected by panoramic radiography and CT: A systematic review and meta-analysis. Dentomaxillofac Radiol 45: 20150310 (2016)

Kamrun N, Tetsumara A, Nomura Y, Yamaguchi S, Baba O, Nakamura S, Watanabe H, Kurabayashi T: Visualization of the superior and inferior borders of the mandibular canal: A comparative study using digital panoramic radiographs and cross-sectional computed tomography images. Oral Surg Oral Med Oral Pathol Oral Radiol 115: 550–557 (2013)

Kang J H, Lee K S, Oh M G, Choi H Y, Lee S R, Oh S H, Choi Y J, Kim G T, Choi Y S, Hwang E H: The incidence and configuration of the bifid mandibular canal in Koreans by using cone-beam computed tomography. Imaging Sci Dent 44: 53–60 (2014)

Kim M S, Yoon S J, Park H W, Kang J H, Yang S Y, Moon Y H, Jung N R, Yoo H I, Oh W M, Kim S H: A false presence of bifid mandibular canals in panoramic radiographs. Dentomaxillofac Radiol 40: 434–438 (2011)

Kovisto T, Ahmad M, Bowles W R: Proximity of the mandibular canal to the tooth apex. J Endod 37: 311–315 (2011)

Krasny A, Krasny N, Prescher A: Anatomic variations of neural canal structures of the mandible observed by 3-tesla magnetic resonance imaging. J Comput Assist Tomogr 36: 150–153 (2012)

Krasny A, Krasny N, Prescher A: Study of inferior dental canal and its contents using high-resolution magnetic resonance imaging. Surg Radiol Anat 34: 687–693 (2012)

Kuribayashi A, Watanabe H, Imaizumi A, Tantanapornkul W, Katakami K, Kurabayashi T: Bifid mandibular canals: Cone beam computed tomography evaluation. Dentomaxillofac Radiol 39: 235–239 (2010)

Langlais R P, Broadus R, Glass B J: Bifid mandibular canals in panoramic radiographs. J Am Dent Assoc 110: 923–926 (1985)

Lew K, Townsend G: Failure to obtain adequate anaesthesia associated with a bifid mandibular canal: A case report. Aust Dent J 51: 86–90 (2006)

Lima Villaca-Carvalho M F, Manhaes Lr J R, de Moraes M E, Lopes S L: Prevalence of bifid mandibular canals by cone beam computed tomography. Oral Maxillofac Surg 20: 289–294 (2016)

Lindgren P, Eriksson K F, Ringberg A: Severe facial ischemia after endodontic treatment. J Oral Maxillofac Surg 60: 576–579 (2002)

Liu T, Xia B, Gu Z: Inferior alveolar canal course: A radiographic study. Clin Oral Implants Res 20: 1212–1218 (2009)

Luangchana P, Pornprasertsuk-Damrongsri S, Kitisubkanchana J, Wongchuensoontorn C: Branching patterns of the inferior alveolar canal in a Thai population: A novel classification using cone beam computed tomography. Quintessence Int 50: 224–231 (2019)

Maqbool A, Sultan A A, Bottini G B, Hopper C: Pain caused by a dental implant impinging on an accessory inferior alveolar canal: A case report. Int J Prosthodont 26: 125–126 (2013)

Naitoh M, Hiraiwa Y, Aimiya H, Ariji E: Observation of bifid mandibular canal using cone-beam computerized tomography. Int J Oral Maxillofac Implants 24: 155–159 (2009)

Naitoh M, Nakahara K, Suenaga Y, Gotoh K, Kondo S, Ariji E: Comparison between cone-beam and multislice computed tomography depicting mandibular neurovascular canal structures. Oral Surg Oral Med Oral Pathol Oral Radiol Endod 109: e25–31 (2010)

Neves F S, Nascimento Mcc, Oliveira M L, Almeida S M, Boscolo F N: Comparative analysis of mandibular anatomical variations between panoramic radiography and cone beam computed tomography. Oral Maxillofac Surg 18: 419–424 (2014)

Nortje C J, Farman A G, Grotepass F W: Variations in the normal anatomy of the inferior dental (mandibular) canal: A retrospective study of panoramic radiographs from 3612 routine dental patients. Br J Oral Surg 15: 55–63 (1977)

Okumus Ö, Dumlu A: Prevalence of bifid mandibular canal according to gender, type and side. J Dent Sci 14: 126–133 (2019)

Orhan K, Aksoy S, Bilecenoglu B, Sakul B U, Paksoy C S: Evaluation of bifid mandibular canals with cone-beam computed tomography in a Turkish adult population: A retrospective study. Surg Radiol Anat 33: 501–507 (2011)

Politis C, Ramirez X B, Sun Y, Lambrichts I, Heath N, Agbaje J O: Visibility of mandibular canal on panoramic radiograph after bilateral sagittal split osteotomy (BSSO). Surg Radiol Anat 35: 233–240 (2013)

Pria C M, Masood F, Beckerley J M, Carson R E: Study of the inferior alveolar canal and mental foramen on digital panoramic images. J Contemp Dent Tract 12: 265–271 (2011)

Rashsuren O, Choi J W, Han W J, Kim E K: Assessment of bifid and trifid mandibular canals using cone-beam computed tomography. Imaging Sci Dent 44: 229–236 (2014)

Serman N: Letter to the Editor. A false presence of bifid mandibular canals in panoramic radiographs. Dentomaxillofac Radiol 41: 620 (2012)

Shah N P, Murtadha L, Brown J: Bifurcation of the inferior dental nerve canal: An anatomical study. Br J Oral Maxillofac Surg 56: 267–271 (2018)

Sharma S, Hackett R, Webb R, Macpherson D, Wilson A: Severe tissue necrosis following intra-arterial injection of endodontic calcium hydroxide: A case series. Oral Surg Oral Med Oral Pathol Oral Radiol Endod 105: 666–669 (2008)

Shen E C, Fu E, Fu M M, Peng M: Configuration and corticalization of the mandibular bifid canal in a Taiwanese adult population: A computed tomography study. Int J Oral Maxillofac Implants 29: 893–897 (2014)

Shen E C, Fu E, Peng M, Hsieh Y D, Tu H P, Fu M W: Bifid mandibular canals and their cortex thicknesses: A comparison study on images obtained from cone-beam and multislice computed tomography. J Dent Sci 11: 170–174 (2016)

Sperber G H: Craniofacial embryology. 3rd edition, J. Wright & Sons Ltd, England (1981)

Verea Linares C, Mohindra A, Evans M: Haemorrhage following coronectomy of an impacted third molar associated with a bifid mandibular canal: A case report and review of the literature. Oral Surg 9: 248–251 (2016)

von Arx T, Bornstein M M, Werder P, Bosshardt D: The retromolar canal (foramen retromolare). Overview and case report (in German). Schweiz Monatsschr Zahnmed 121: 821–834 (2011)

Von Arx T, Lozanoff S: Clinical Oral Anatomy – A Comprehensive Review for Dental Practitioners and Researchers. 1st edition, Springer International, Switzerland (2017)

Wilbrand J F, Wilbrand M, Schaaf H, Howaldt H P, Malik C Y, Streckbein P: Embolia cutis medicamentosa (Nicolau Syndrome) after endodontic treatment: A case report. J Endod 37: 875–877 (2011)

Yamada T, Ishihama K, Yasuda K, Hasumi-Nakayama Y, Ito K, Yamaoka M, Furusawa K: Inferior alveolar nerve canal and branches detected with dental cone beam computed tomography in lower third molar region. J Oral Maxillofac Surg 69: 1278–1282 (2011)

Yang X, Lyu C, Zou D: Bifid mandibular canals incidence and anatomical variations in the population of Shanghai area by cone beam computed tomography. J Comput Assist Tomogr 41: 535–540 (2017)

Yoon Tyh, Robinson D K, Estrin N E, Tagg D T, Michaud R A, Dinh T N: Utilization of cone beam computed tomography to determine the prevalence and anatomical characteristics of bifurcated inferior alveolar nerves. Gen Dent 66: 22–26 (2018)

Zhang Y Q, Zhao Y N, Liu D G, Meng Y, Ma X C: Bifid variations of the mandibular canal: Cone beam computed tomography evaluation of 1000 northern Chinese patients. Oral Surg Oral Med Oral Pathol Oral Radiol 126: e271–278 (2018)

Zhou X, Gao X, Zhang J: Bifid mandibular canals: CBCT assessment and macroscopic observation. Surg Radiol Anat 42: 1073–1079 (2020)